

# MoQE: Improve Quantization Model performance via Mixture of Quantization Experts.

Jinhao Zhang<sup>1</sup> Yunquan Zhang<sup>2</sup> Boyang Zhang<sup>3,4</sup> Zeyu Liu<sup>5</sup> Daning Cheng<sup>2</sup>

<sup>1</sup>Beijing University of Posts and Telecommunications, Beijing, China

<sup>2</sup>Institute of Computing Technology, Chinese Academy of Sciences, Beijing, China

<sup>3</sup>University of Chinese Academy of Sciences, Beijing, China

<sup>4</sup>Peng Cheng Laboratory, Shenzhen, China

<sup>5</sup>North University of China, Taiyuan, China

## Abstract

Quantization method plays a crucial role in improving model efficiency and reducing deployment costs, enabling the widespread application of deep learning models on resource-constrained devices. However, the quantization process inevitably introduces accuracy degradation. In this paper, we propose Mixture of Quantization Experts( abbr. MoQE), a quantization inference framework based on the Mixture-of-Experts (MoE) architecture, aiming to jointly improve the performance of quantization models. MoQE combines multiple quantization variants of one full-precision model as specialized "quantization experts" and dynamically routes input data to the most suitable expert based on its characteristics. MoQE alleviates the performance degradation commonly seen in single quantization models through specialization quantization expert models. We design lightweight, structure-aware router models tailored for both CV and NLP tasks. Experimental evaluations on ResNet, LLaMA, and Qwen model families across benchmark datasets including ImageNet, WikiText, C4, and OpenWebText demonstrate that MoQE achieves performance comparable to SOTA quantization model, without incurring significant increases in inference latency.

## Introduction

Quantization method plays a pivotal role in the field of machine learning, particularly in enhancing model efficiency and reducing resource consumption. As deep learning models grow increasingly complex, their demand for computational resources escalates, constraining deployment on resource-limited devices and increasing operational costs. Quantization mitigates storage requirements and computational complexity by reducing the precision of model weights and activations. Furthermore, Quantization method streamlines the model optimization pipeline, enabling developers to achieve efficient deployment within shorter timeframes and accelerating time-to-market for AI-driven products. Consequently, Quantization method serves not only as a critical enabler for improving the accessibility and practicality of machine learning models but also as a key facilitator in the broader dissemination of artificial intelligence technologies.

Copyright © 2026, Association for the Advancement of Artificial Intelligence (www.aaai.org). All rights reserved.

Quantization techniques exhibit notable advantages in compressing deep neural network models and minimizing computational overhead. However, their practical deployment faces several critical challenges. Quantization inherently involves mapping high-precision floating-point parameters to low-bit representations, a process that inevitably introduces information loss, thereby degrading model generalization and accuracy. This degradation is particularly pronounced under ultra-low bit-width settings (e.g., below 8 bits), where quantization noise can significantly impair representational capacity, leading to performance deterioration—especially in complex tasks or applications with stringent accuracy requirements. Thus, achieving high efficiency without compromising model performance remains a central research challenge.

The MoE (Mixture of Experts) system is an artificial intelligence architecture based on a combination of expert models, designed to solve complex problems by integrating the capabilities of multiple specialized models (the "experts"). Each expert handles a specific aspect of the input data, while a component called the "gating network" determines how to allocate tasks to different experts based on the input's characteristics. We named gating network as router model in this paper. This approach allows the model to scale to very large sizes while maintaining computational efficiency, as not all experts need to compute every input. MoE systems are particularly suitable for applications requiring high flexibility and strong expressive power, such as NLP and image recognition, delivering more accurate and personalized services and predictions. As technology advances, MoE has become a key technique for building efficient, large-scale machine learning models. However, there are few works which focus on how to improve quantization model performance via MoE system.

To mitigate the performance degradation caused by model quantization, make full use of computing resources, and avoid significantly decreasing the inference speed of the quantization model, we propose Mixture of Quantization Expert methods (MoQE)—an expert system for quantization inference based on the MoE paradigm. Prior studies (Liu et al. 2025) indicate that different quantization variants of the same full-precision model exhibit heterogeneous performance degradation across distinct sub-datasets. Motivated

by this observation, MoQE assigns different sub-datasets to specialized quantization models—termed “quantization experts”—thereby improving the overall system performance. Notably, as the number of quantization experts increases, the coverage and representational diversity of the system expand, leading to progressive performance gains.

To facilitate dynamic routing of input data to appropriate quantization experts, we design two router models tailored respectively for CV and NLP models. These routers leverage key structural components from their respective base models, ensuring compatibility and semantic relevance, while maintaining a significantly smaller scale to ensure rapid execution with minimal computational overhead.

We evaluate MoQE using ResNet, LLaMA, and Qwen series models on benchmark datasets including ImageNet, WikiText, C4, and OpenWebText. Experimental results demonstrate that MoQE consistently achieves performance comparable to that of the best individual quantization model, without incurring significant increases in inference latency.

Our contributions are listed as the following:

1. We design a Mixture of Quantized Experts system, abbr. MoQE. By integrating quantization models into an expert system, MoQE routes different data subsets to the quantization models where they perform best, resulting in overall system performance superior to that of any single expert.

2. We design data router models for both CV and NLP tasks. The router model is a lightweight classification model with a short inference time, achieving inference speed of MoQE system comparable to that of a single quantization model.

3. Through experiments, we have validated the performance of MoQE on both CV and NLP tasks. Experimental results show that the performance of the MoQE system exceeds that of any individual quantization expert model comprising it. Furthermore, the performance of the MoQE system improves as the number of expert models increases. And experiments code address is shown in the Appendix.

## Related Works

**Quantization** is one of the most popular techniques for compressing neural networks. It can be roughly divided into two main methods: quantization-aware training (QAT) and post-training quantization (PTQ). QAT considers quantization during the network training phase, while PTQ quantizes the network after training. PTQ is widely used in network deployment due to its low time consumption and computational resource requirements. HAWQ-v2 (Dong et al. 2019) uses the trace of the layer weight’s Hessian matrix as the index to show this layer’s sensitivity. The work (Zhe et al. 2019) formulates the mixed-precision problem of weights and activations as a Lagrangian optimization problem whose solution is the optimum joint precision allocation for all weights and activations. AdaQuant (Hubara et al. 2020) optimizes its parameters on the calibration set to minimize the quantization error of each layer separately. (Liu et al. 2023) alleviate the overfitting problem in PTQ caused by the small number of calibration sets by adjusting the distribution of activations. (Shang et al. 2024) introduced mutual information

into PTQ calibration to optimize the quantization parameters. These methods focus on the quantization parameters to alleviate the quantization error, but cannot achieve good results at very low bits and run slowly. Our method uses performance and speed improvements at very low bits, and does not require calibration sets and fine-tuning.

**Mixture of Experts (MoE)** (Jacobs et al. 1991; Eigen, Ranzato, and Sutskever 2013) is a composite modeling framework comprising multiple specialized sub-models, referred to as experts, which are combined through a structured integration mechanism. There are two kinds of MoE paradigm hard routers and soft router. In the hard routing paradigm, experts are typically pre-assigned to handle specific, predefined patterns or modalities. This design choice is motivated by the inherent disparities among multi-modal data (Liang et al. 2022), which can hinder soft routing mechanisms from effectively learning optimal token-to-expert assignment policies. A number of studies (Bao et al. 2022; Long et al. 2023; Shen et al. 2023) exploit this modality-level separation by explicitly decoupling experts according to data modalities, with each expert dedicated to processing a single modality. A key advantage of such hard routing approaches is that they eliminate the need for training or learning the router, simplifying deployment. This strategy has also been widely adopted in task-specific MoE architectures (Li et al. 2023; Ma et al. 2023). In contrast, soft routers have been extensively explored in NLP (Shazeer et al. 2017; Fedus, Zoph, and Shazeer 2022; Komatsuzaki et al. 2022; Zoph et al. 2022), where routing decisions are made probabilistically, enabling dynamic and context-aware allocation of tokens to different experts. This flexibility allows each expert to specialize in particular semantic or syntactic patterns, promoting model sparsity and scalability. Our work primarily focuses on leveraging soft routing mechanisms within the MoE framework. Notably, soft-routed MoE architectures have also been adapted to multimodal learning in smaller-scale models (e.g., million-parameter range), such as EVE (Chen et al. 2024) and LIMoE (Mustafa et al. 2022), which utilize soft routers to facilitate cross-modal fusion.

## Methodological Mixture of Quantization Experts

To mitigate the degradation of model accuracy caused by quantization, this paper proposes a novel framework termed Mixture of Quantization Experts (MoQE), the working pattern of MoQE is shown in Figure 1. In the MoQE architecture, multiple quantization variants of the same full-precision model are integrated through an expert system paradigm. These quantization models are typically derived via different quantization methods on the same full-precision model. The selection of which specific quantization model to activate is governed by a dedicated router model. The design and formulation of the router model will be detailed in the following section. The activated quantization expert model performs the inference on this sample. The router model is trained by a train dataset.

The theoretical foundation of this approach stems from the observation that different quantization models exhibit

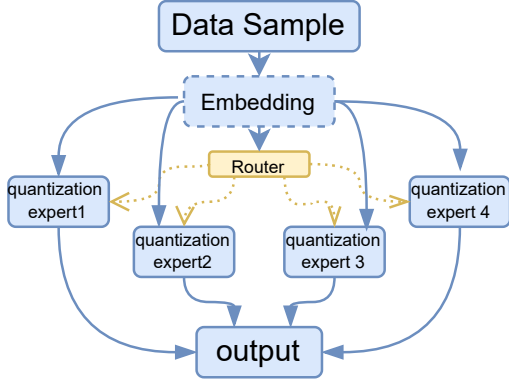


Figure 1: The working pattern of MoQE. The data sample first passes through a router model which may involve embedding process, to determine which quantization expert model to activate, and then is fed into the corresponding quantization expert model for inference.

distinct biases (unfairness) across various regions of the input data space (Liu et al. 2025). Specifically, for certain subsets of data, one quantization model may consistently yield lower prediction errors (i.e., lower loss values) than others. By leveraging the router model to dynamically assign samples to the most suitable expert, MoQE effectively selects, at each inference step, the model with the lowest loss function value on this subset of data. As illustrated in the Figure 2, this strategy enables the system to synthesize a composite decision boundary that outperforms any individual quantization model. Consequently, the router model can be interpreted as a multi-class classifier, and its effective design is critical to ensuring that the overall system performance exceeds that of any constituent model.

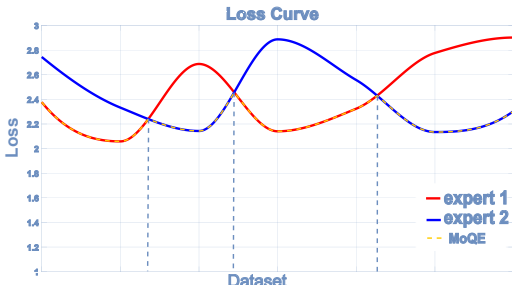


Figure 2: The explanations of MoQE system which consists of two quantization experts. MoQE always selects the model with the lower loss on this subset of data.

It is important to note that the router model operates on vectorized representations of input data, implying that raw data formats may first be transformed into appropriate embedding. This process is optional depending on the tasks. For example, in CV tasks, images are naturally represented as tensors and can be directly processed by the router model. Thus, CV tasks do not need embedding process. In contrast, for NLP tasks, textual inputs must be converted into dense vector representations—typically through embedding tech-

niques—before they can be handled. The quality of this embedding process directly influences the router model’s classification accuracy.

In the context of NLP, MoQE uses the pre-existing embedding layer of the original full-precision model as its embedding layer. This choice serves two purposes: (1) it avoids the need to train a separate embedding layer for routing, which would be computationally expensive and potentially degrade performance due to misalignment; and (2) reducing inference cost, using the same embedding layer saves one inference step through the embedding layer. Therefore, the embedding layer of the quantization expert models is not quantized.

In our experimental design, we primarily focus on quantization variants of a single full-precision model, reflecting typical industrial deployment scenarios where only one full-precision model is available for quantization. Moreover, in NLP tasks, the shared embedding layer constraint limits the framework to experts originating from the same base model, which limits that all quantization expert models are from the same full-precision model. However, the MoQE framework is, in principle, extensible to quantization models derived from multiple distinct full-precision models. Prior work (Liu et al. 2025) suggests that for well-trained models, performance variations across quantization versions in different data regions are largely determined by local gradient and Hessian matrix properties.

## Router Model

The design of router models must be tailored to the intrinsic characteristics of different task domains. For instance, NLP tasks necessitate a strong emphasis on contextual dependencies, while CV tasks primarily rely on spatial and hierarchical visual features. By carefully calibrating the architectural and parametric configurations of the router model, classification accuracy can be significantly improved, ensuring that each quantization expert model operates at peak efficacy within its targeted data distribution. This, in turn, contributes to enhanced overall inference accuracy.

Accordingly, in the development of task-specific routing architectures, we advocate for the reconstruction of foundational components based on domain-informed models. This strategy ensures heightened sensitivity and adaptability to the unique statistical and semantic properties of the input data within a given modality. To this end, and to address the prevalent use cases in modern deep learning, we have designed two specialized router models tailored specifically for CV and NLP tasks, respectively—each optimized to exploit the structural priors inherent in its respective domain.

**CV Router Model** We present a lightweight, multi-head ResNet-8 router model for computer vision (CV) tasks that resolves the load-imbalance and computational redundancy endemic to conventional multi-expert architectures. The pipeline begins with an MLP that compresses a 2048-D global feature into  $1024 \rightarrow 128 \rightarrow 1024$  dimensions, each followed by batch normalization (BN) and ReLU activation. The resulting 1024-D vector is reshaped into a  $48 \times 16 \times 8 \times 8$  tensor, preserving fine-grained spatial cues while remaining

amenable to efficient convolution. A three-stage SEResNet-8 (with channel dimensions 16/32/64, stride pattern  $1 \rightarrow 2 \rightarrow 2$ , and one BasicBlock per stage) then extracts local representations. Finally, the feature map is flattened into a sequence and fed to an 8-head self-attention module (head dimension 8, learnable temperature  $\tau = 1.0$ ) to yield the routing logits, ensuring globally-aware yet balanced expert assignment with minimal overhead.

**NLP Router Model** The core design principle of our router model in the NLP Router is to endow routing decisions with the same level of semantic richness and contextual sensitivity as the expert computations themselves. Conventional router model typically apply only a single linear transformation to token embeddings, which inherently restricts their receptive field to a local, context-agnostic perspective. This limitation often results in ambiguous or sub-optimal routing, as tokens—deprived of their broader linguistic context—may be misclassified. To overcome this, we propose a deep, hierarchical context-aware router that systematically enriches token representations through multiple stages of contextual processing. The structure of router model is shown in Figure 3.

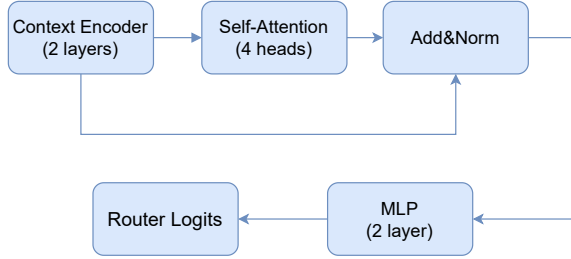


Figure 3: The structure of router model

The foundation of our architecture is a multi-layer Transformer encoder, configured with two layers (`transformer_layers=2`), each equipped with four attention heads (`nhead=4`), a feed-forward dimension of twice the embedding size (`dim_feedforward=2×embed_dim`), GELU non-linearity, and a dropout rate of 0.1. The encoder employs pre-layer normalization (`norm_first=True`) and operates in batch-first mode (`batch_first=True`). It will convert the entire sequence in parallel, replacing the static token embeddings with representations that reflect the context, thereby capturing the linguistic environment around each token.

Subsequent to this initial contextual encoding, we introduce a dedicated self-attention module designed for context refinement and selective focus. This module comprises independent linear projections for query, key, and value (each of dimension `embed_dim`), with attention scores scaled by  $\sqrt{embed\_dim/num\_heads}$ . It further incorporates attention dropout (`attn_drop=0.1`), a projection layer (`proj`), projection dropout (`proj_drop=0.1`), and a final layer normalization (`norm`). Far from being redundant, this stage functions as a context-aware refinement mechanism, enabling the model to dynamically re-weight the relevance

of different contextual elements in determining the optimal routing path for each token.

The resulting representations are then passed through a final multilayer perceptron (MLP) to compute routing logits. This MLP consists of a dimensionality reduction layer (`embed_dim → embed_dim/2`), followed by GELU activation, dropout, and a linear projection to the number of experts (`num_experts`). This multi-stage processing pipeline—encompassing global contextual encoding, context refinement via self-attention, and non-linear score generation—ensures that routing decisions are grounded in a comprehensive and fine-grained understanding of the input's semantic intent.

Nevertheless, a complex router model necessitates a robust stabilization framework to prevent pathological behaviors such as *expert collapse*, a common failure mode in which only a small subset of experts is consistently activated. To mitigate this, we implement a comprehensive, multi-faceted load-balancing strategy comprising three key components:

1. An explicit load-balancing loss term that encourages uniform expert utilization within each batch;
2. Dynamic, history-aware bias adjustment, wherein expert usage frequencies are tracked via an exponential moving average (EMA, decay factor  $\alpha = 0.8$ ), and a negative bias proportional to utilization is applied to discourage overuse (scaled by a balance strength coefficient of 0.8);
3. Controlled noise injection during training, involving soft additive noise governed by a learnable parameter (`noise_epsilon=1.0`), combined with temperature-scaled softmax (gating\_temperature = 1.0). This noise is gradually annealed during training to balance exploration and convergence.

## MoQE and Parallel Inference

In the broader context of inference frameworks, particularly beyond the scope of quantization, a critical challenge emerges: simply scaling up the number of GPUs does not always lead to a faster inference speed when model is inferring a single sample. Unlike traditional parallel computing paradigms, where increased hardware resources typically translate to faster execution, inference workloads often fail to benefit proportionally from additional GPUs. This is primarily because the inference process is constrained by the model's architectural design and its inherent degree of parallelism. As a result, adding more GPUs can lead to underutilization of computational resources. Furthermore, the overhead associated with inter-device communication and synchronization can exacerbate inefficiencies, potentially degrading overall system performance rather than improving it.

In contrast to the conventional paradigm of trading computational resources for reduced inference latency, MoQE introduces a novel approach that leverages increased computational resources to improve inference quality—manifested as lower PPL in NLP tasks or higher classification accuracy in CV tasks. By adopting the MoE deployment strategy employed in DeepSeek, distinct quantization experts can be dis-

tributed across different computational devices. DeepSeek MoE deployment strategy keeps low inference latency. As our analysis demonstrates, the integration of a growing number of quantization expert models for specific data subsets enhances overall system performance while simultaneously enabling more effective utilization of hardware resources. This scalability in model experts offers a promising direction for achieving higher accuracy without compromising inference speed.

In addressing large-scale parallel inference tasks, conventional approaches rely on data parallelism by replicating a single quantization model across devices. This strategy effectively scales throughput through hardware augmentation.

The MoQE system presents a paradigm shift by introducing a quantization expert ensemble architecture with dynamic routing. Three key innovations enable better performance than data parallelism:

**Decoupled Execution:** Independent operation of quantization experts eliminates model-sharing bottlenecks, achieving data-parallel-like throughput through true parallelism.

**Lightweight Routing:** Sample-specific routing decisions incur minimal overhead while maintaining independence across processing units. When the same router model infers different samples, the inference processes are independent. Therefore, data parallelism can be applied to the routing model's inference without affecting overall performance.

**Experts-Driven Optimization:** By assigning each sample to the most suitable expert based on data characteristics, the system maximizes model performance without compromising inference speed.

A workload-balanced MoQE system not only matches the throughput of data parallelism but also outperforms it in model accuracy. This dual advantage stems from its ability to simultaneously optimize for both computational efficiency and system performance.

## Experiments

The experiments in this chapter will demonstrate the performance of the MoQE system. The experiments are divided into three parts. In CV tasks, the primary models are those based on residual architectures, specifically the ResNet and MobileNet series. In NLP tasks, our main focus is on current mainstream large language models, namely the Qwen and Llama series. Finally, we will analyze the relationship between the different system configurations and system performance, which we use as an ablation experiment.

### CV Experiments

**Experiments Configurations** The experiments configurations are listed as the following:

**Model** We use standard ResNet50, ResNet101, and MobileNetV2 as the experimental models. 8-bit integer (Int8) quantization is applied in this section.

**Router Training Setting** In training the router model, the same hyperparameter settings for the Adam optimizer were used across different backbone networks: the learning rate is set to  $5.00 \times 10^{-5}$  for all models, the learning rate schedule employs cosine annealing, the batch size was set to 48,

gradient accumulation over 2 steps was applied, and weight decay was set to 0. Additional training details are provided in the Appendix.

**Benchmarks and MoQE Setting.** In our experiments, we use BRECQ (Li et al. 2021), DSConv (Nascimento, Prisacariu, and Fawcett 2020), N2UQ (Liu et al. 2021), and a QAT-trained model. The quantization expert models in MoQE consist of the above-mentioned benchmark models.

We present the performance of MoQE when the quantization expert models are not derived from the same full-precision model.

**Dataset** We use the ImageNet dataset, which remains a cornerstone in computer vision and is widely recognized as a benchmark for image classification and visual representation learning. It comprises over one million annotated images across 1,000 semantic categories.

Acc	ResNet50	ResNet101	MobileNetV2
BRECQ	76.44%	77.60%	69.10%
QAT	77.09%	77.50%	71.10%
N2UQ	76.40%	78.30%	71.11%
DSConv	76.08%	77.90%	70.32%
MoQE(Our)	78.01%	78.91%	71.36%
FP16	80.21%	83.25%	71.80%

Table 1: Performance Comparison between the MoQE System and Individual Expert Models in CV Tasks

**Experimental Results Analysis** The experimental results are shown in Table 1. As can be observed from the experimental results in Table 1, the MoQE system demonstrates consistently superior performance across various quantization schemes on both ResNet and MobileNet series models. Overall, MoQE effectively mitigates the accuracy degradation typically induced by quantization while maintaining model efficiency.

A detailed analysis reveals the following: On ResNet50, MoQE achieves an accuracy of 78.01%, significantly outperforming BRECQ (76.44%) and DSConv (76.08%), and slightly surpassing N2UQ (76.40%) and QAT (77.09%). This indicates that MoQE more effectively preserves the performance of the original FP16 model (80.21%). The advantage of MoQE becomes even more pronounced on the deeper ResNet101, where it attains an accuracy of 78.91%. This result is notably higher than those of BRECQ (77.60%) and QAT (77.50%), and also exceeds the performance of N2UQ (78.30%) and DSConv (77.90%), fully demonstrating MoQE's robustness and effectiveness in handling complex models. For the lightweight MobileNet model, although the performance gap among different methods is relatively small, MoQE still achieves the best result with an accuracy of 71.36%, outperforming BRECQ (69.10%), QAT (71.10%), N2UQ (71.11%), and DSConv (70.32%), and closely approaching the original FP16 model's accuracy of 71.80%.

In summary, the MoQE system exhibits consistent and superior quantization performance across CV models with varying architectures and complexities. It maximizes the preservation of model accuracy at the Int8 quantization

level, outperforming mainstream quantization approaches such as post-training quantization (PTQ), quantization-aware training (QAT), and other specialized methods (e.g., BRECQ, N2UQ and DSConv). These results validate the effectiveness of MoQE as a high-efficiency quantization framework.

## NLP Experiments

**Experiment Configurations** The experiment configurations are listed as follows:

**Model** We use standard Qwen-0.6B, Qwen-1.7B, Qwen-4B, and Llama-3B as our experimental models. Int8 quantization is applied in this section.

**Router Training Setting** During training of the router model, the Adam optimizer hyperparameter settings are kept consistent across different model scales: the learning rate is set to  $5.00 \times 10^{-5}$  for all models, the cosine learning rate scheduler is employed, the batch size is 8, gradient accumulation is applied with 6 steps, and the weight decay coefficient is set to 0.01. Additional training details are provided in the Appendix.

**Benchmarks and MoQE Setting** In our experiments, we use SmoothQuant (Xiao et al. 2023), GPTQ (Frantar et al. 2022), Imatrix, and K-quantization. To evaluate the impact of the number of experts, we additionally include AWQ (Lin et al. 2024) as a benchmark in the configuration (Ablation) experiments. The quantization expert models in MoQE consist of the above-mentioned benchmark models.

**Dataset** We use the C4, WikiText-2, and OpenWebText datasets to evaluate our algorithm. C4, a cleaned version of Common Crawl filtered for quality, assesses model robustness on noisy, real-world web text. WikiText-2, composed of structured Wikipedia articles, provides a standard benchmark for evaluating perplexity and modeling long-range dependencies. OpenWebText, a corpus of user-endorsed online content, tests the model’s ability to generate fluent, human-preferred text. These datasets are widely used in language modeling benchmark. In the following, we abbreviate WikiText-2 as Wiki and OpenWebText as WebText.

**Experimental Results Analysis** The experimental results are shown in Table 2. As shown in Table 2, the experimental results demonstrate the performance of the MoQE system across various large language models (Qwen0.6B, Qwen1.7B, Llama3B, and Qwen4B) and multiple NLP datasets (C4, WikiText-2, and OpenWebText). The evaluation metric is perplexity (lower is better), and MoQE is compared against several state-of-the-art quantization methods, including GPTQ, SmoothQuant, K-Quants, and imatrix, with FP16 serving as the full-precision baseline.

Overall, MoQE consistently achieves the lowest perplexity across nearly all model sizes and datasets, indicating its superior ability to preserve language modeling performance under quantization. Notably, MoQE not only outperforms all other quantization methods but also significantly closes the gap with the full-precision FP16 models. For instance, on the Qwen0.6B model, MoQE achieves perplexities of 24.82 (C4), 20.16 (WikiText-2), and 18.97 (OpenWebText), which are substantially lower than those of the

next best method (imatrix) and much closer to the FP16 baseline (17.18, 12.76, 11.32) than any other quantization approach.

This trend persists across larger models. On Qwen1.7B, MoQE obtains 18.13 (C4), 15.97 (WikiText-2), and 14.02 (OpenWebText), again outperforming all competitors and demonstrating strong scalability. In the case of Llama3B and Qwen4B, MoQE achieves the most significant gains—on Llama3B/OpenWebText, MoQE reaches a perplexity of 10.03, surpassing even the FP16 baseline (11.57), which may be attributed to regularization effects induced by the MoE router model. Similarly, on Qwen4B, MoQE achieves 15.94 (C4), 13.69 (WikiText-2), and 12.89 (OpenWebText), significantly outperforming other quantization methods and approaching or exceeding FP16 performance on certain tasks.

These results validate that the MoQE framework effectively combines the strengths of multiple quantization experts through intelligent routing, minimizing quantization-induced degradation. Its consistent superiority across diverse architectures and datasets underscores its robustness and generalizability, making it a highly effective solution for deploying large language models under resource-constrained conditions.

## Ablation Experiment

**Int4 Experts** In this section, we will present the impact of various quantization level on the MoQE system. We use Int4 quantization models to build MoQE system. The experimental results are shown in Table 3.

As shown in Table 3, this experiment evaluates the performance of the MoQE system employing various Int4 quantization methods as experts on the Qwen series models (0.6B, 1.7B, 4B). The evaluation metric is perplexity (lower is better), and the results are compared with those of individual quantization methods and the full-precision FP16 model.

The experimental results indicate that the MoQE framework still exhibits significant advantages at the Int4 quantization level. Across all tested models and datasets, MoQE achieves the lowest perplexity, significantly outperforming each individual quantization method. Specifically, on the Qwen0.6B model, MoQE attains perplexities of 31.98 (C4) and 31.67 (WikiText-2), which are not only lower than those of GPTQ (33.12, 32.12), K-Quants (37.87, 36.53), imatrix (34.68, 34.15), and SmoothQuant (49.58, 47.21), but also closer to the FP16 baseline (17.18, 12.76). This indicates that MoQE can effectively mitigate the severe performance degradation caused by Int4 quantization in smaller models.

This advantage is equally pronounced in larger-scale models. On the Qwen1.7B, MoQE achieves perplexities of 21.72 (C4) and 20.44 (WikiText-2), surpassing all baseline methods, including the relatively better-performing imatrix (27.32, 27.89) and K-Quants (23.44, 25.32). Notably, on the Qwen4B model with even larger parameter sizes, MoQE’s advantage becomes more prominent, with perplexities of 17.09 (C4) and 13.89 (WikiText-2), which not only significantly outperform other quantization methods but also exhibit the smallest gap relative to the FP16 baseline (11.84, 7.95). This demonstrates the MoQE framework’s enhanced

PPL	Qwen0.6			Qwen1.7B			Llama3B			Qwen4B		
	C4	WiKi	webtext	C4	WiKi	webtext	C4	WiKi	webtext	C4	WiKi	webtext
GPTQ	25.63	21.07	19.76	19.32	16.85	14.96	16.87	14.30	13.87	19.37	14.47	13.66
SmoothQuant	25.94	22.11	20.34	18.96	16.73	15.08	17.69	15.17	12.13	16.71	22.45	20.97
K-Quants	32.38	24.54	21.68	21.40	17.58	16.31	17.34	15.21	15.14	21.45	17.34	15.44
imatrix	27.84	26.38	22.45	19.24	18.54	16.38	12.18	11.82	10.93	18.32	19.89	16.38
MoQE(Our)	24.82	20.16	18.97	18.13	15.97	14.02	11.54	11.01	10.03	15.94	13.69	12.89
FP16	17.18	12.76	11.32	13.48	9.53	9.02	13.56	12.46	11.57	11.84	7.95	6.35

Table 2: Performance Comparison between the MoQE System and Individual Expert Models in NLP Tasks

PPL	Qwen0.6		Qwen1.7B		Qwen4B	
	C4	WiKi	C4	WiKi	C4	WiKi
GPTQ	33.12	32.12	22.19	21.05	20.06	14.53
SmoothQuant	49.58	47.21	30.28	29.55	17.53	22.43
K-Quants	37.87	36.53	23.44	25.32	25.47	16.78
imatrix	34.68	34.15	27.32	27.89	21.32	18.32
MoQE(Our)	31.98	31.67	21.72	20.44	17.09	13.89
FP16	17.18	12.76	13.48	9.53	11.84	7.95

Table 3: MoQE System with Int4 Quantization Experts

robustness and higher accuracy retention when handling large models under Int4 quantization.

In summary, the MoQE system successfully overcomes the limitations of individual quantization methods by effectively integrating the predictive capabilities of multiple Int4 quantization experts. It maximizes the preservation of the original model’s language understanding and generation abilities while maintaining a high degree of model compression. The consistent superior performance across different scales of Qwen models fully validates the effectiveness and scalability of this framework in extreme quantization (Int4) scenarios.

Furthermore, by comparing Table 2, we observe that after employing Int4 quantization models, the perplexity (ppl) of the individual quantization experts increases, consequently leading to a performance degradation in the MoQE system composed of Int4 experts. However, it is evident that even under these conditions, MoQE still achieves the best performance among all the models evaluated.

**Number of Experts** In this section, we investigate the impact of varying the number of experts on the performance of the MoQE system. We further employ the AWQ algorithm to quantize the original full-precision model and incorporate it as a new expert into the MoQE framework. The augmented system is then trained, and the results are presented in the following Table 4.

As shown in Table 4, we extend the MoQE system by incorporating AWQ as an additional quantization expert, resulting in a total of five experts (GPTQ, SmoothQuant, K-Quants, imatrix, and AWQ). The performance of the individual AWQ expert and the aggregated MoQE system is analyzed below.

The AWQ method performs competitively among the individual quantization approaches, achieving perplexities of 25.54 (C4) and 21.04 (WikiText-2) on Qwen0.6B, and 19.23

PPL	Qwen0.6		Qwen1.7B	
	C4	WiKi	C4	WiKi
GPTQ	25.63	21.07	19.32	16.85
SmoothQuant	25.94	22.11	18.96	16.73
K-Quants	32.38	24.54	21.40	17.58
imatrix	27.84	26.38	19.24	18.54
AWQ	25.54	21.04	19.23	16.78
MoQE(Our)	24.69	19.62	18.01	15.86
FP16	17.18	12.76	13.48	9.53

Table 4: MoQE system with Five Quantization Experts

(C4) and 16.78 (WikiText-2) on Qwen1.7B. These results are slightly better than GPTQ and SmoothQuant, indicating AWQ’s effectiveness in preserving model accuracy under Int8 quantization.

More importantly, the MoQE system, which integrates routing over all five experts including AWQ, achieves the lowest perplexity across both models and datasets: 24.69 (C4) and 19.62 (WikiText-2) for Qwen0.6B, and 18.01 (C4) and 15.86 (WikiText-2) for Qwen1.7B. This demonstrates that the inclusion of AWQ as an expert further enhances the representational capacity of the ensemble, enabling the gating network to leverage complementary strengths across diverse quantization strategies. The superior performance of MoQE confirms that the dynamic expert selection mechanism effectively combines the best aspects of each method—particularly benefiting from AWQ’s strong baseline performance—thereby minimizing quantization error and outperforming even the best individual expert (AWQ) in all cases. This validates the scalability and robustness of the MoQE framework when extended to a larger set of heterogeneous quantization experts.

## Conclusion

This paper addresses the issue of performance degradation in quantization models by proposing the MoQE system. This framework integrates multiple quantization models and routes input data to the model with the smallest performance degradation, thereby ensuring that the system’s overall output surpasses that of any individual quantization expert models. We design distinct router models for CV and NLP tasks. Since inference involves only one quantization model and the router model is relatively small, the overall inference performance is not significantly impacted. Experiments demonstrate that the performance of the MoQE system exceeds that of any single quantization expert within the system.

## References

Bao, H.; Wang, W.; Dong, L.; Liu, Q.; Mohammed, O. K.; Aggarwal, K.; Som, S.; Piao, S.; and Wei, F. 2022. Vlmo: Unified vision-language pre-training with mixture-of-modality-experts. *Advances in neural information processing systems*, 35: 32897–32912.

Chen, J.; Guo, L.; Sun, J.; Shao, S.; Yuan, Z.; Lin, L.; and Zhang, D. 2024. Eve: Efficient vision-language pre-training with masked prediction and modality-aware moe. In *Proceedings of the AAAI Conference on Artificial Intelligence*, volume 38, 1110–1119.

Dong, Z.; Yao, Z.; Gholami, A.; Mahoney, M.; and Keutzer, K. 2019. HAWQ: Hessian AWare Quantization of Neural Networks with Mixed-Precision. *IEEE*.

Eigen, D.; Ranzato, M.; and Sutskever, I. 2013. Learning factored representations in a deep mixture of experts. *arXiv preprint arXiv:1312.4314*.

Fedus, W.; Zoph, B.; and Shazeer, N. 2022. Switch transformers: Scaling to trillion parameter models with simple and efficient sparsity. *Journal of Machine Learning Research*, 23(120): 1–39.

Frantar, E.; Ashkboos, S.; Hoefer, T.; and Alistarh, D. 2022. Gptq: Accurate post-training quantization for generative pre-trained transformers. *arXiv preprint arXiv:2210.17323*.

Hubara, I.; Nahshan, Y.; Hanani, Y.; Banner, R.; and Soudry, D. 2020. Improving post training neural quantization: Layer-wise calibration and integer programming. *arXiv preprint arXiv:2006.10518*.

Jacobs, R. A.; Jordan, M. I.; Nowlan, S. J.; and Hinton, G. E. 1991. Adaptive mixtures of local experts. *Neural computation*, 3(1): 79–87.

Komatsuzaki, A.; Puigcerver, J.; Lee-Thorp, J.; Ruiz, C. R.; Mustafa, B.; Ainslie, J.; Tay, Y.; Dehghani, M.; and Houlsby, N. 2022. Sparse upcycling: Training mixture-of-experts from dense checkpoints. *arXiv preprint arXiv:2212.05055*.

Li, Y.; Gong, R.; Tan, X.; Yang, Y.; and Gu, S. 2021. BRECQ: Pushing the Limit of Post-Training Quantization by Block Reconstruction.

Li, Y.; Hui, B.; Yin, Z.; Yang, M.; Huang, F.; and Li, Y. 2023. Pace: Unified multi-modal dialogue pre-training with progressive and compositional experts. *arXiv preprint arXiv:2305.14839*.

Liang, V. W.; Zhang, Y.; Kwon, Y.; Yeung, S.; and Zou, J. Y. 2022. Mind the gap: Understanding the modality gap in multi-modal contrastive representation learning. *Advances in Neural Information Processing Systems*, 35: 17612–17625.

Lin, J.; Tang, J.; Tang, H.; Yang, S.; Chen, W.-M.; Wang, W.-C.; Xiao, G.; Dang, X.; Gan, C.; and Han, S. 2024. Awq: Activation-aware weight quantization for on-device llm compression and acceleration. *Proceedings of machine learning and systems*, 6: 87–100.

Liu, B.; Miao, W.; Zhang, B.; Zhang, Q.; Yuan, B.; Wang, J.; Liu, S.; and Deng, X. 2025. Understanding the Unfairness in Network Quantization. In *Forty-second International Conference on Machine Learning*.

Liu, J.; Niu, L.; Yuan, Z.; Yang, D.; Wang, X.; and Liu, W. 2023. Pd-quant: Post-training quantization based on prediction difference metric. In *Proceedings of the IEEE/CVF Conference on Computer Vision and Pattern Recognition*, 24427–24437.

Liu, Z.; Cheng, K. T.; Huang, D.; Xing, E.; and Shen, Z. 2021. Nonuniform-to-Uniform Quantization: Towards Accurate Quantization via Generalized Straight-Through Estimation. *arXiv e-prints*.

Long, Z.; Killick, G.; McCreadie, R.; and Camarasa, G. A. 2023. Multiway-adapater: Adapting large-scale multi-modal models for scalable image-text retrieval. *arXiv preprint arXiv:2309.01516*.

Ma, G.; Wu, X.; Wang, P.; and Hu, S. 2023. Cot-mote: exploring contextual masked auto-encoder pre-training with mixture-of-textual-experts for passage retrieval. *arXiv preprint arXiv:2304.10195*.

Mustafa, B.; Riquelme, C.; Puigcerver, J.; Jenatton, R.; and Houlsby, N. 2022. Multimodal contrastive learning with limoe: the language-image mixture of experts. *Advances in Neural Information Processing Systems*, 35: 9564–9576.

Nascimento, M. G. D.; Prisacariu, V.; and Fawcett, R. 2020. DSCConv: Efficient Convolution Operator. *IEEE*.

Shang, Y.; Liu, G.; Kompella, R. R.; and Yan, Y. 2024. Enhancing Post-training Quantization Calibration through Contrastive Learning. In *Proceedings of the IEEE/CVF Conference on Computer Vision and Pattern Recognition*, 15921–15930.

Shazeer, N.; Mirhoseini, A.; Maziarz, K.; Davis, A.; Le, Q.; Hinton, G.; and Dean, J. 2017. Outrageously large neural networks: The sparsely-gated mixture-of-experts layer. *arXiv preprint arXiv:1701.06538*.

Shen, S.; Yao, Z.; Li, C.; Darrell, T.; Keutzer, K.; and He, Y. 2023. Scaling vision-language models with sparse mixture of experts. *arXiv preprint arXiv:2303.07226*.

Xiao, G.; Lin, J.; Seznec, M.; Wu, H.; Demouth, J.; and Han, S. 2023. Smoothquant: Accurate and efficient post-training quantization for large language models. In *International conference on machine learning*, 38087–38099. PMLR.

Zhe, W.; Lin, J.; Chandrasekhar, V.; and Girod, B. 2019. Optimizing the Bit Allocation for Compression of Weights and Activations of Deep Neural Networks. In *2019 IEEE International Conference on Image Processing (ICIP)*.

Zoph, B.; Bello, I.; Kumar, S.; Du, N.; Huang, Y.; Dean, J.; Shazeer, N.; and Fedus, W. 2022. St-moe: Designing stable and transferable sparse expert models. *arXiv preprint arXiv:2202.08906*.

## Reproducibility Checklist

### 1. General Paper Structure

1.1. Includes a conceptual outline and/or pseudocode description of AI methods introduced (yes/partial/no/NA) **yes**

- 1.2. Clearly delineates statements that are opinions, hypothesis, and speculation from objective facts and results (yes/no) **yes**
- 1.3. Provides well-marked pedagogical references for less-familiar readers to gain background necessary to replicate the paper (yes/no) **yes**

## 2. Theoretical Contributions

- 2.1. Does this paper make theoretical contributions? (yes/no) **yes**

If yes, please address the following points:

- 2.2. All assumptions and restrictions are stated clearly and formally (yes/partial/no) **yes**
- 2.3. All novel claims are stated formally (e.g., in theorem statements) (yes/partial/no) **yes**
- 2.4. Proofs of all novel claims are included (yes/partial/no) **yes**
- 2.5. Proof sketches or intuitions are given for complex and/or novel results (yes/partial/no) **yes**
- 2.6. Appropriate citations to theoretical tools used are given (yes/partial/no) **yes**
- 2.7. All theoretical claims are demonstrated empirically to hold (yes/partial/no/NA) **yes**
- 2.8. All experimental code used to eliminate or disprove claims is included (yes/no/NA) **no**

## 3. Dataset Usage

- 3.1. Does this paper rely on one or more datasets? (yes/no) **yes**

If yes, please address the following points:

- 3.2. A motivation is given for why the experiments are conducted on the selected datasets (yes/partial/no/NA) **yes**
- 3.3. All novel datasets introduced in this paper are included in a data appendix (yes/partial/no/NA) **NA**
- 3.4. All novel datasets introduced in this paper will be made publicly available upon publication of the paper with a license that allows free usage for research purposes (yes/partial/no/NA) **yes**
- 3.5. All datasets drawn from the existing literature (potentially including authors' own previously published work) are accompanied by appropriate citations (yes/no/NA) **yes**
- 3.6. All datasets drawn from the existing literature (potentially including authors' own previously published work) are publicly available (yes/partial/no/NA) **yes**

- 3.7. All datasets that are not publicly available are described in detail, with explanation why publicly available alternatives are not scientifically satisfying (yes/partial/no/NA) **NA**

## 4. Computational Experiments

- 4.1. Does this paper include computational experiments? (yes/no) **yes**

If yes, please address the following points:

- 4.2. This paper states the number and range of values tried per (hyper-) parameter during development of the paper, along with the criterion used for selecting the final parameter setting (yes/partial/no/NA) **yes**
- 4.3. Any code required for pre-processing data is included in the appendix (yes/partial/no) **yes**
- 4.4. All source code required for conducting and analyzing the experiments is included in a code appendix (yes/partial/no) **yes**
- 4.5. All source code required for conducting and analyzing the experiments will be made publicly available upon publication of the paper with a license that allows free usage for research purposes (yes/partial/no) **yes**
- 4.6. All source code implementing new methods have comments detailing the implementation, with references to the paper where each step comes from (yes/partial/no) **yes**
- 4.7. If an algorithm depends on randomness, then the method used for setting seeds is described in a way sufficient to allow replication of results (yes/partial/no/NA) **NA**
- 4.8. This paper specifies the computing infrastructure used for running experiments (hardware and software), including GPU/CPU models; amount of memory; operating system; names and versions of relevant software libraries and frameworks (yes/partial/no) **yes**
- 4.9. This paper formally describes evaluation metrics used and explains the motivation for choosing these metrics (yes/partial/no) **partial**
- 4.10. This paper states the number of algorithm runs used to compute each reported result (yes/no) **no**
- 4.11. Analysis of experiments goes beyond single-dimensional summaries of performance (e.g., average; median) to include measures of variation, confidence, or other distributional information (yes/no) **no**
- 4.12. The significance of any improvement or decrease in performance is judged using appropriate statistical

tests (e.g., Wilcoxon signed-rank) (yes/partial/no) **no**

4.13. This paper lists all final (hyper-)parameters used  
for each model/algorithm in the paper's experiments  
(yes/partial/no/NA) **yes**